

## Chemical Constituents and Anti-Neuroblastoma Activity from *Boesenbergia stenophylla*

(Sebatian Kimia dan Aktiviti Anti-Neuroblastoma daripada *Boesenbergia stenophylla*)

PHOEBE SUSSANA PRIMUS<sup>1</sup>, MUHAMMAD HAZRAN ISMAIL<sup>1</sup>, NABILA ELYANA ADNAN<sup>1</sup>, CAROL HSIN-YI WU<sup>2</sup>,  
CHAI-LIN KAO<sup>3</sup> & YEUN-MUN CHOO<sup>1,\*</sup>

<sup>1</sup>Department of Chemistry, Faculty of Science, University of Malaya, 50603 Kuala Lumpur, Federal Territory, Malaysia

<sup>2</sup>Division of Cellular and Immune Therapy, Department of Medical Research, Kaohsiung Medical University Hospital, Kaohsiung Medical University, Taiwan

<sup>3</sup>Department of Medicinal and Applied Chemistry, Kaohsiung Medical University, Taiwan

Received: 5 May 2021/Accepted: 6 September 2021

### ABSTRACT

Three diarylheptanoids and one flavonoid, i.e. 7-(4-hydroxy-3-methoxyphenyl)-1-phenylhept-4-en-3-one (**4**), 5R-hydroxy-7-(4-hydroxy-3-methoxyphenyl)-1-phenylheptan-3-one (**5**), 1,7-diphenylhept-4-en-3-one (**6**), and 3,5,7-trihydroxyflavone (**7**) were isolated and characterized from the rhizome of *Boesenbergia stenophylla*. Compounds **2** and **4** displayed excellent anti-neuroblastoma activity which reduces the cell viability to 30% and 20%, respectively. The results from the molecular docking experiments targeting the protein kinases regulating neuroblastoma cell survival (PI3K/AKT1 signalling pathway) are consistent with that of the *in vitro* results. Finally, the structures of **4-7** were elucidated using spectroscopic methods (UV, IR, NMR, and HRESIMS).

Keywords: AKT1; anti-neuroblastoma; *Boesenbergia stenophylla*; N2A; PI3K

### ABSTRAK

Tiga diarilheptanoid dan satu flavonoid, iaitu, 7-(4-hidroksi-3-metoksifenil)-1-fenilhept-4-en-3-on (**4**), 5R-hidroksi-7-(4-hidroksi-3-metoksifenil)-1-fenilheptan-3-on (**5**), 1,7-difenilhept-4-en-3-on (**6**) dan 3,5,7-trihidroksiflavon (**7**) daripada akar *Boesenbergia stenophylla* telah diasingkan dan dikenal pasti. Sebatian **2** dan **4** mempunyai aktiviti anti-neuroblastoma dan ia berjaya merencatkan keviabelan sel masing-masing kepada 30% dan 20%. Hasil kajian daripada dok molekul secara *in silico* yang disasarkan kepada protein kinase yang mengawal atur kewujudan sel neuroblastoma (laluan isyarat PI3K/AKT1) ini adalah sejajar dengan hasil kajian *in vitro*. Akhir sekali, struktur sebatian **4-7** telah ditentukan dengan menggunakan kaedah spektroskopi (UV, IR, NMR dan HREIMS) dan perbandingan dengan data literatur.

Kata kunci: AKT1; anti-neuroblastom; *Boesenbergia stenophylla*; N2A; PI3K

### INTRODUCTION

*Boesenbergia stenophylla* is a lesser-known ginger from Malaysia, belonging to the Zingiberaceae. The *Boesenbergia* consists of about 70 species found in the tropical Asia region (Ahmad & Jantan 2003; Ling et al. 2010; Mustahil 2009; Newman et al. 2004; Saensouk & Larsen 2001; Tewtrakul et al. 2003; Tuchinda et al. 2002). *B. stenophylla*, has been utilized for protection against convulsions, prevention of intoxication, cough

relief, increase libido, and treatment of food poisoning (Ahmad & Jantan 2003; Ling et al. 2010; Noor Atiekah & Halijah). Previous reports have shown that *Boesenbergia* spp. contains diverse chemical constituents, such as flavonoids, diarylheptanoid, phenolic acids, terpenoids, and steroids; and has shown promising biological activities such as anti-inflammatory, antibacterial, antiviral, analgesic, and antioxidant (Ling et al. 2010; Noor Atiekah & Halijah 2018; Sudsai et al. 2014; Tewtrakul et al. 2003;

Tuchinda et al. 2002). However, very little information on *B. stenophylla* such as the chemical constituents and bioactivities are available in the literatures. We have recently reported three new compounds (**1-3**) from *B. stenophylla* (Primus et al. 2021) and we wish to report four more compounds from the same plant, i.e. 7-(4-hydroxy-3-methoxyphenyl)-1-phenylhept-4-en-3-one (**4**), 5*R*-hydroxy-7-(4-hydroxy-3-methoxyphenyl)-

1-phenylheptan-3-one (**5**), 1,7-diphenylhept-4-en-3-one (**6**), and 3,5,7-trihydroxyflavone (**7**) (Figure 1), and anti-neuroblastoma activity from *B. stenophylla* rhizome. Compounds **2**, **4**, and **6** were subjected to *in vitro* neuroblastoma cell viability assay. Molecular docking experiments were carried out on compounds **1-7** to evaluate its binding affinities and interactions with the protein kinases regulating neuroblastoma cell survival.

#### EXPERIMENTAL DETAILS

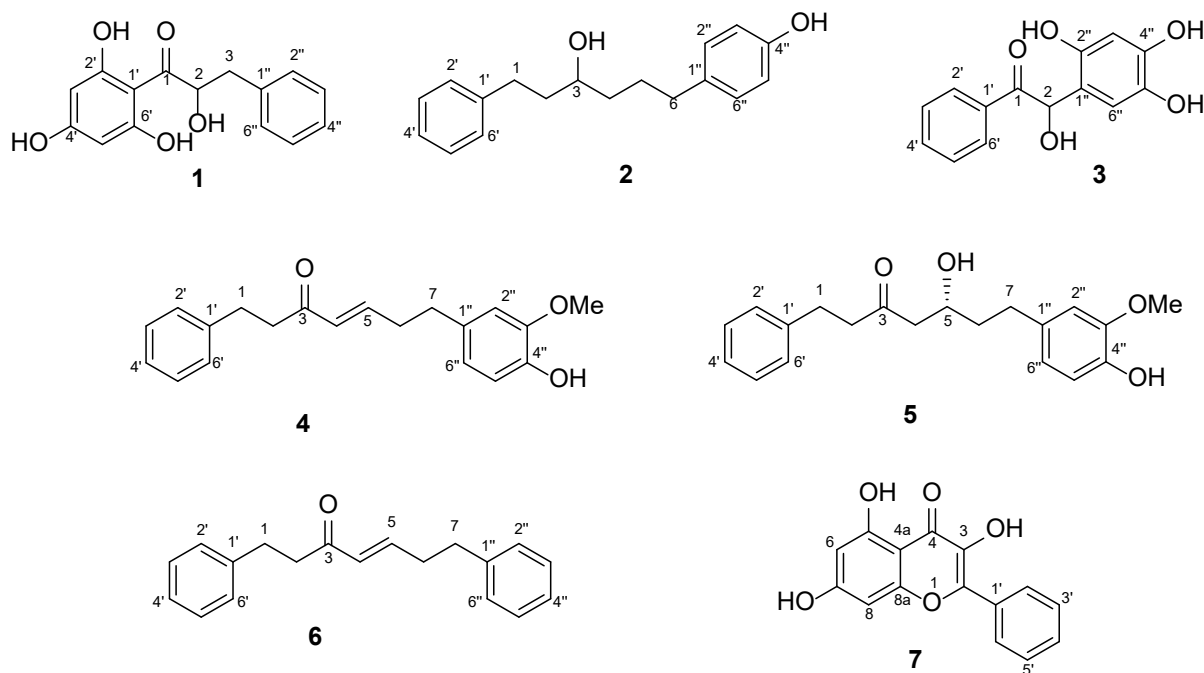


FIGURE 1. Compounds **1-7**

#### GENERAL

Bruker AVANCE III 600 MHz spectrometer was used to record the NMR spectra. Agilent 6530 Q-TOF (Agilent Technologies, Santa Clara, CA, USA) mass spectrometer coupled to Agilent 1200 series Rapid Resolution LC system was used to obtain the HRESIMS data. PerkinElmer 1760x FT-IR spectrophotometer was used to record IR spectra. Agilent Cary 60 UV Vis spectrophotometer (Agilent Technologies, Santa Clara, CA, USA) was used for UV measurement. JASCO P-1020 polarimeter (JASCO Corporation) was used for optical rotation measurements. All solvents used in this study were from Fisher Brand (AR grade, Loughborough, Leicestershire, UK).

#### PLANT MATERIAL, EXTRACTION AND ISOLATION

*Boesenbergia stenophylla* was obtained from Alor Setar, Kedah, Malaysia. A voucher of the specimen (UM-092012-B009) is available at the herbarium of the Chemistry Department, University of Malaya, Kuala Lumpur, Malaysia. The crude hexane (3.8 g),  $\text{CHCl}_3$  (2.4 g), and EtOH (105.1 g) extracts were obtained from the sequential soaking of the dried-ground rhizome (1.0 kg) with hexane,  $\text{CHCl}_3$ , and 95% EtOH.

Silica gel 60 (0.040-0.063, Merck, Darmstadt, Germany) was used for column chromatography (CC; 70×3 cm) and Kieselgel 60 with gypsum (Merck, Darmstadt, Germany) was used for centrifugal chromatography (CFC). CC ( $\text{CHCl}_3$  100%) on the  $\text{CHCl}_3$  extract yielded fraction C1-C3. CFC ( $\text{CHCl}_3$  100%) of C1 and C2 yielded **1** (13.6 mg) and **5** (41.9 mg); and **3** (51.0 mg), respectively. CFC ( $\text{CHCl}_3$ :MeOH 98:2) of C3 yielded **2** (15.7 mg). CC

(hexane:CHCl<sub>3</sub> 1:1 followed by hexane:diethyl ether 4:6) on the hexane extract yielded fraction H1 and H2. CFC (hexane:diethyl ether 2:8) of H2 yielded **4** (15.9 mg). CC (CHCl<sub>3</sub> 100%) on the EtOH extract yielded fraction E1 and E2. Further CC purification (hexane:CHCl<sub>3</sub>

1:1) of E1 gave fraction E1-1. Sequential CFC of E1-1 (hexane:CHCl<sub>3</sub> 8:2 followed by 100% CHCl<sub>3</sub>) yielded **6** (13.5 mg). Sequential CFC of E2 (hexane:CHCl<sub>3</sub> 1:1 followed by 100% CHCl<sub>3</sub>) yielded **7** (1.0 mg).

TABLE 1. <sup>1</sup>H (CDCl<sub>3</sub>, 600 MHz) and <sup>13</sup>C NMR (CDCl<sub>3</sub>, 125 MHz) NMR spectroscopic data (δ) of compounds **4-6**

Position	<b>4</b>		<b>5</b>		<b>6</b>	
	δ <sub>H</sub>	δ <sub>C</sub>	δ <sub>H</sub>	δ <sub>C</sub>	δ <sub>H</sub>	δ <sub>C</sub>
1	2.92 t (8)	30.0	2.87 t (8)	29.5	2.92 t (8)	30.2
2	2.84 t (8)	41.9	2.72 t (8)	45.0	2.84 t (8)	41.9
3	-	199.6	-	211.1	-	199.6
4	6.11 d (16)	130.8	2.53 m	49.3	6.11 dt (15, 1)	130.9
5	6.83 m	146.5	4.04 m	67.0	6.84 dt (15,7)	146.4
6	2.49 q (8)	34.6	1.76 m 1.63 m	38.4	2.53 ddd (15,7,1)	34.3
7	2.69 t (8)	34.3	2.70 m 2.58 m	31.4	2.76 dt (15,7)	34.6
1'	-	141.4	-	140.7	-	141.4
2'	7.19 d (7)	128.5	7.14 d (8)	128.3	7.19 m	126.7
3'	7.27 t (7)	128.6	7.26 t (8)	128.5	7.28 m	128.5
4'	7.20 t (7)	126.2	7.18 t (8)	126.2	7.19 m	128.5
5'	7.27 t (7)	128.6	7.26 t (8)	128.5	7.28 m	128.5
6'	7.19 d (7)	128.5	7.14 d (8)	128.3	7.19 m	126.7
1''	-	132.7	-	133.7	-	140.8
2''	6.65 m	115.5	6.68 s	111.3	7.19 m	126.7
3''	-	146.6	-	146.6	7.28 m	128.5
4''	-	144.1	-	143.8	7.19 m	128.5
5''	6.83 m	114.5	6.81, d (7)	114.5	7.28 m	128.5
6''	6.65 m	121.0	6.65 d (7)	120.9	7.19 m	126.7
3''-OMe	3.85 s	56.0	3.82 s	55.9	-	-

7-(4-HYDROXY-3-METHOXYPHENYL)-1-PHENYLHEPT-4-EN-3-ONE (**4**)

Dark brown oil; molecular formula C<sub>20</sub>H<sub>22</sub>O<sub>3</sub>; UV (MeOH) λ<sub>max</sub> (log ε) 224 (3.76), 282 (3.20), 371 (2.54) nm; IR (NaCl) ν<sub>max</sub> 3422, 2936, 1686, 1656, 1515, 1272 cm<sup>-1</sup>. <sup>1</sup>H NMR and <sup>13</sup>C NMR: Table 1. HRESIMS *m/z* 309.1752 [M-H]<sup>-</sup> (calcd for C<sub>20</sub>H<sub>21</sub>O<sub>3</sub><sup>-</sup>, 309.1728) and 293.1808 [M-OH]<sup>-</sup> (calcd for C<sub>20</sub>H<sub>21</sub>O<sub>3</sub><sup>-</sup>, 293.1779).

5R-HYDROXY-7-(4-HYDROXY-3-METHOXYPHENYL)-1-PHENYLHEPTAN-3-ONE (**5**)

Dark brown oil; molecular formula C<sub>20</sub>H<sub>24</sub>O<sub>4</sub>; [α]<sub>D</sub> -14.5 (c 0.0159, CHCl<sub>3</sub>); UV (MeOH) λ<sub>max</sub> (log ε) 274 (3.33) nm; IR (NaCl) ν<sub>max</sub> 3430, 2938, 1714 and 1270 cm<sup>-1</sup>. <sup>1</sup>H NMR and <sup>13</sup>C NMR: Table 1. HRESIMS *m/z* 327.1596 [M-H]<sup>-</sup> (calcd for C<sub>20</sub>H<sub>23</sub>O<sub>4</sub><sup>-</sup>, 327.1614) and 351.1572 [M+Na]<sup>+</sup> (calcd for C<sub>20</sub>H<sub>24</sub>O<sub>4</sub>Na<sup>+</sup>, 327.1550).

## 1,7-DIPHENYLHEPT-4-EN-3-ONE (6)

Light yellow oil; molecular formula  $C_{19}H_{20}O$ ; UV (MeOH)  $\lambda_{\max}$  (log  $\epsilon$ ) 210 (3.47), 245 (2.90), 280 (2.41) nm; IR (NaCl)  $\nu_{\max}$  2955, 1708 and 973  $cm^{-1}$ ;  $^1H$  NMR and  $^{13}C$  NMR: Table 1. HRESIMS  $m/z$  283.1791  $[M+H+H_2O]^+$  (calcd for  $C_{19}H_{22}O_2^+$ , 283.1698).

## 3,5,7-TRIHYDROXYFLAVONE (7)

Light yellow oil; molecular formula  $C_{15}H_{10}O_5$ ; UV (MeOH)  $\lambda_{\max}$  (log  $\epsilon$ ) 213 (3.62), 269 (3.45), 318 (3.12), 367 (3.19) nm; IR (NaCl)  $\nu_{\max}$  3352, 2362 and 1599  $cm^{-1}$ ;  $^1H$  NMR ( $CDCl_3$ , 600 MHz)  $\delta$  7.38 (2H, d,  $J=8.0$  Hz, H-2' and H-6'), 6.69 (2H, t,  $J=8.0$  Hz, H-3' and H-5'), 6.64 (H, t,  $J=8.0$  Hz, H-4'), 5.61 (1H, s, H-8), 5.40 (1H, s, H-6).  $^{13}C$  NMR ( $CDCl_3$ , 125 MHz)  $\delta$  158.2 (C, C-5), 156.5 (C, C-7), 153.1 (C, C-8a), 137.7 (C, C-2), 123.2 (C, C-1'), 121.6 (CH, C-4'), 120.1 (2CH, C-3' and C-5'), 119.4 (2CH, C-2' and C-6'), 94.9 (C, C-4a), 90.1 (CH, C-8), 84.6 (CH, C-6). HRESIMS  $m/z$  269.0481  $[M-H]^-$  (calcd for  $C_{15}H_9O_5^-$ , 269.0455).

## NEUROBLASTOMA CELL VIABILITY ASSAY

Culture media for N2A cell: Dulbecco's modified Eagle's medium (DMEM, Gibco BRL, Life Technologies Inc., USA), 10% fetal bovine serum, 100  $\mu g/mL$  penicillin, 100  $\mu g/mL$  streptomycin, and in a humidified atmosphere containing 5%  $CO_2$  at 37  $^{\circ}C$ . The test compound (triplicate) and N2A cells culture were incubated in a 96-well plate ( $5.0 \times 10^3$  cells per well) for 24 h. Cell Counting Kit-8 (CCK-8; Dojindo Molecular Technologies, Japan) was used to measure cell viability by adding 10  $\mu L$  of CCK-8 solution to each well at the time-points of 24 h. Optical density (OD) was recorded with a plate reader at 450 nm (Thermo Scientific™ Multiskan™ GO Microplate Spectrophotometer) after incubation period of 3 h at 37  $^{\circ}C$ . The survival rate was calculated using the formula described below and analyzed using Microsoft Excel software.

Cell Survival Rate % = (drug stimulation cells OD/control group cells OD)  $\times$  100%.

## MOLECULAR DOCKING

The structures of **1-7** were optimized using the MM2 energy-minimized function in the Chem3D Ultra version 16.0. The crystal structure of the receptor proteins, i.e. AKT1 (PDB ID: 4EKK, x-center = 13.685, y-center = 1.377, z-center = 19.389), PI3K (PDB ID: 4FA6, x-center

= 44.555, y-center = 13.306, z-center = 31.313), ALK (PDB ID: 3LCS, x-center = -20.292, y-center = 11.084, z-center = -8.376), and FAK (PDB ID: 2IJM, z-center = 2.031, y-center = 6.656, z-center = 6.756), were obtained from Protein Data Bank (Berman et al. 2000; Burley et al. 2019). AutoDockTools version 1.5.6 were used to prepare the receptor proteins and ligands for the molecular docking experiment. The grid box parameter used are: grid box spacing = 1.0  $\text{\AA}$ ; x-dimension = y-dimension = z-dimension = 20. AutoDock Vina programme was used to perform the docking and calculate the binding affinity (Sanner 1999; Trott & Olson 2010). And lastly, the results were processed and analysed using the BIOVIA Discovery Studio Visualizer version 17.2.0.

## RESULTS AND DISCUSSION

The NMR spectral of compounds **4-6** are highly similar suggesting the presence of the diarylheptanoid core skeleton. The IR spectra of **4** showed the presence of hydroxyl (3422  $cm^{-1}$ ), carbonyl (1686  $cm^{-1}$ ), and ether (1272  $cm^{-1}$ ) functional groups. The molecular formula of **4** ( $C_{20}H_{22}O_3$ ) is confirmed by HRESIMS with the observation of  $m/z$  309.1752  $[M-H]^-$  and 293.1808  $[M-OH]^-$ . The COSY spectrum of **4** indicated the presence of unsubstituted aryl, *m,p*-disubstituted aryl,  $-CH_2CH_2-$  and  $-CH=CHCH_2CH_2-$  partial structures. The observed coupling constant for H(4)/H(5) (16 Hz) suggested the C(4)=C(5) double bond adopts the *E* configuration. The HMBC spectrum confirmed the structure of the middle seven-membered alkyl-chain through  $J^{\beta}$  correlations from C(3) carbonyl to H(1) and H(5); and from C(7) to H(5). The position of the aryl groups are confirmed through  $J^{\beta}$  HMBC correlations from C(1) to H(2') and H(6'); and C(7) to H(2'') and H(6''), while the position of the OMe group is confirmed by  $J^{\beta}$  HMBC correlation from C(3'') to OMe. The observed  $J^{\beta}$  HMBC correlations between C(4'') with H(2'') and H(6'') and  $J^{\alpha}$  HMBC correlation from C(4'') to H(5''); coupled with the observation of  $\delta_{C-4''}$ , 144.1 suggested the presence of a hydroxyl substitution at C(4''). Hence, the structure of **4** is deduced as (*E*)-7-(4-hydroxy-3-methoxyphenyl)-1-phenylhept-4-en-3-one and the experimental data of **4** is in agreement with the literature (Itokawa et al. 1981).

Compound **5** was obtained as dark brown oil with  $[\alpha]_D -14.5$  (*c* 0.0159,  $CHCl_3$ ). The HRESIMS showed  $m/z$  327.1596  $[M-H]^-$  and 351.1572  $[M+Na]^+$  in ESI-negative and ESI-positive mode, respectively, confirming the molecular formula  $C_{20}H_{24}O_4$ . The NMR and IR spectra of **5** is similar to that of **4**. The alkene signals ( $\delta_{H-4}$  6.11 and

$\delta_{C-4}$  130.8;  $\delta_{H-5}$  6.83 and  $\delta_{C-5}$  146.5) in the NMR spectra of **4** has been replaced by the methylene-hydroxyl function ( $\delta_{H-4}$  2.53 and  $\delta_{C-4}$  49.3;  $\delta_{H-5}$  4.04, and  $\delta_{C-5}$  67.0) in **5** suggesting the 5-hydroxy-7-(4-hydroxy-3-methoxyphenyl)-1-phenylheptan-3-one structure for **5**. The IR spectrum showed a hydroxyl signal at 3430  $\text{cm}^{-1}$ , while the oxymethine signal was observed at  $\delta_C$  67.0 ( $\delta_H$  4.04) in the NMR spectral. The configuration of the 5-OH was confirmed to be *R*, consistent with the  $[\alpha]_D$  value reported in the literature (experimental  $[\alpha]_D$  -14.5; literature  $[\alpha]_D$  -12.1) (Gamre et al. 2021).

1,7-Diphenylhept-4-en-3-one (**6**) is the last diarylheptanoid isolated in the present study. It was obtained as light yellow oil with a molecular formula of  $\text{C}_{19}\text{H}_{20}\text{O}$ . The NMR spectra of **6** is consistent with literature report (Tori et al. 1995), showing the presence of two unsubstituted aryl rings observed at  $\delta_H$  7.19 (integrated for six protons and assigned to H2', H2'', H4', H4'', H6' and H6'') and 7.28 (integrated for four protons and assigned to H3', H3'', H5', and H5'') connected by a hep-4-en-3-one middle chain.

3,5,7-Trihydroxyflavone (**7**) was isolated in very small amounts as light yellow oil and displayed primarily low-field  $^1\text{H}$  NMR signals attributed to the aryl protons. The  $^{13}\text{C}$  NMR spectrum also showed primarily low-field signals indicating the presence of a ketone and multiple hydroxyl-substituted  $sp^2$  quaternary carbons, in addition to the aryl carbons. The experimental data of **7** (NMR, IR, and MS) were identical with galagin (Afolayan & Meyer 1997), a common flavone, thus confirming the identity of **7**.

Neuroblastoma is accounted for over 15% of children cancer related death (Greengard 2018; London et al. 2005; Maris et al. 2007; Megison et al. 2013). Due to the small amount of compounds isolated, only compounds **2**, **4**, and **6** were tested on the neuroblastoma cells and the results are summarized in Figure 2 and Table 1. Compounds **4** and **2** were shown to be able to reduce neuroblastoma cell viability to 20 and 30% in 24 h, respectively, suggesting their potential as anti-neuroblastoma agents. The anti-neuroblastoma activity assigned to **4** has been erroneously reported as **1** in our earlier publication (Primus et al. 2021) and we wish to make the correction in the present report.

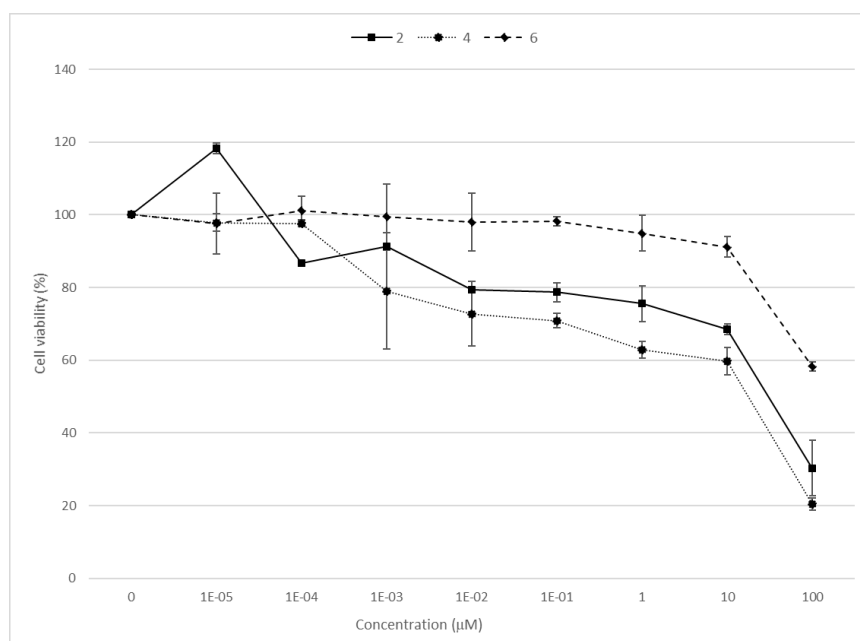


FIGURE 2. Neuroblastoma cell viability of **2**, **4**, and **6**

TABLE 2. Neuroblastoma cell viability and binding affinity (kcal/mol)

	Cell viability (%)	PI3K	AKT1	ALK	FAK
1	n.a.	-6.9	-7.4	-7.3	-7.5
2	30.3±7.4	-7.3	-8.3	-7.1	-6.8
3	n.a.	-6.8	-7.3	-7.1	-7.8
4	20.4±1.7	-7.8	-8	-7.5	-7.5
5	n.a.	-7.5	-7.8	-7.3	-7.4
6	58.3±1.3	-7.5	-8.6	-7.3	-7.4
7	n.a.	-7.7	-7.9	-8.5	-8.1
ATP	n.a.	-7.1	-7.8	-8.3	-8.7

n.a. - not available

Encouraged by the favourable *in vitro* results, deeper understanding on the possible target in neuroblastoma cell signaling pathway by these compounds would provide valuable information for future development (Bahmad et al. 2019; Megison et al. 2013). One of the important groups of protein regulating neuroblastoma cell survival are the protein kinases (Megison et al. 2013). Small molecules have been demonstrated to effectively inhibit the kinases' functions by binding at the ATP-site (Gross et al. 2015; Jänne et al. 2009). Among the key kinases involved in neuroblastoma cell regulation are phosphoinositide 3-kinase (PI3K), RAC- $\alpha$  serine/threonine-protein kinase (AKT1), anaplastic lymphoma kinase (ALK), and focal adhesion kinase (FAK). The PI3K/AKT1 pathway has been shown to play an important role in human cancer cell survival including neuroblastoma (Hennesy et al. 2005; Johnsen et al. 2008). ALK is an upstream signaling kinase of AKT1 and has been showed as effective treatment target for controlling the proliferation of neuroblastoma (Grosso et al. 2011). FAK is a non-receptor tyrosine kinase regulating cell proliferation, viability, and survival (Gabarra-Niecko et al. 2003). Previous studies have shown that inhibiting these protein kinases resulted in the decrease of neuroblastoma cells survival (Megison et al. 2013).

Under the constraint of access to the physical compounds, the *in silico* experiment offers an opportunity for deeper insight on the possible pathway responsible for the activity in greater detail. We have performed

molecular docking to evaluate the binding affinity of **1-7** with the protein kinases responsible in neuroblastoma cells survival (Table 2). Compounds **1-7** were docked at the ATP-binding domain using previously described methods (Karan et al. 2020). The calculated binding affinities of **1-7** were compared against that of ATP to determine its potential as protein kinase inhibitor. The results showed that most compounds (except **1** and **3**) bind better to AKT1 and PI3K than ATP (Figure 3). In the case of ALK and FAK, ATP displayed better binding affinity than most tested compounds. The molecular docking results suggested compounds **2** and **4-7** potential as AKT1- and PI3K-inhibitor. The observed anti-neuroblastoma effect of **2** and **4** in *in vitro* assay could be possibly due to the inhibitory effect against PI3K and/or AKT1 as suggested in the *in silico* experiments. Detailed analysis on the binding configurations of **2** and **4** to PI3K and AKT1 showed a few interesting observations (Figure 4). Both of the aryl groups in **2** and **4** formed multiple interactions with the amino acid residues at the binding pocket. However, compound **4** formed an additional interaction which is absent in **2**, i.e. interaction between the carbonyl function with the amino acid residue at the binding pocket. The analysis also showed that compound **4** formed more interactions with the amino acid residues at the binding pocket than that of **2** and ATP, in both PI3K and AKT1. It is reasonable to conclude that 1) the aryl groups of the diarylheptanoid structure were essential for interactions with the amino acid residues at the binding pocket; 2) methoxy and/or hydroxy substitutions on the

aryl group provided more opportunity for interactions, especially the hydrogen-bonding type; 3) the carbonyl

function at the heptyl middle-chain is able to provide an additional site for interaction, further strengthen the binding interaction.

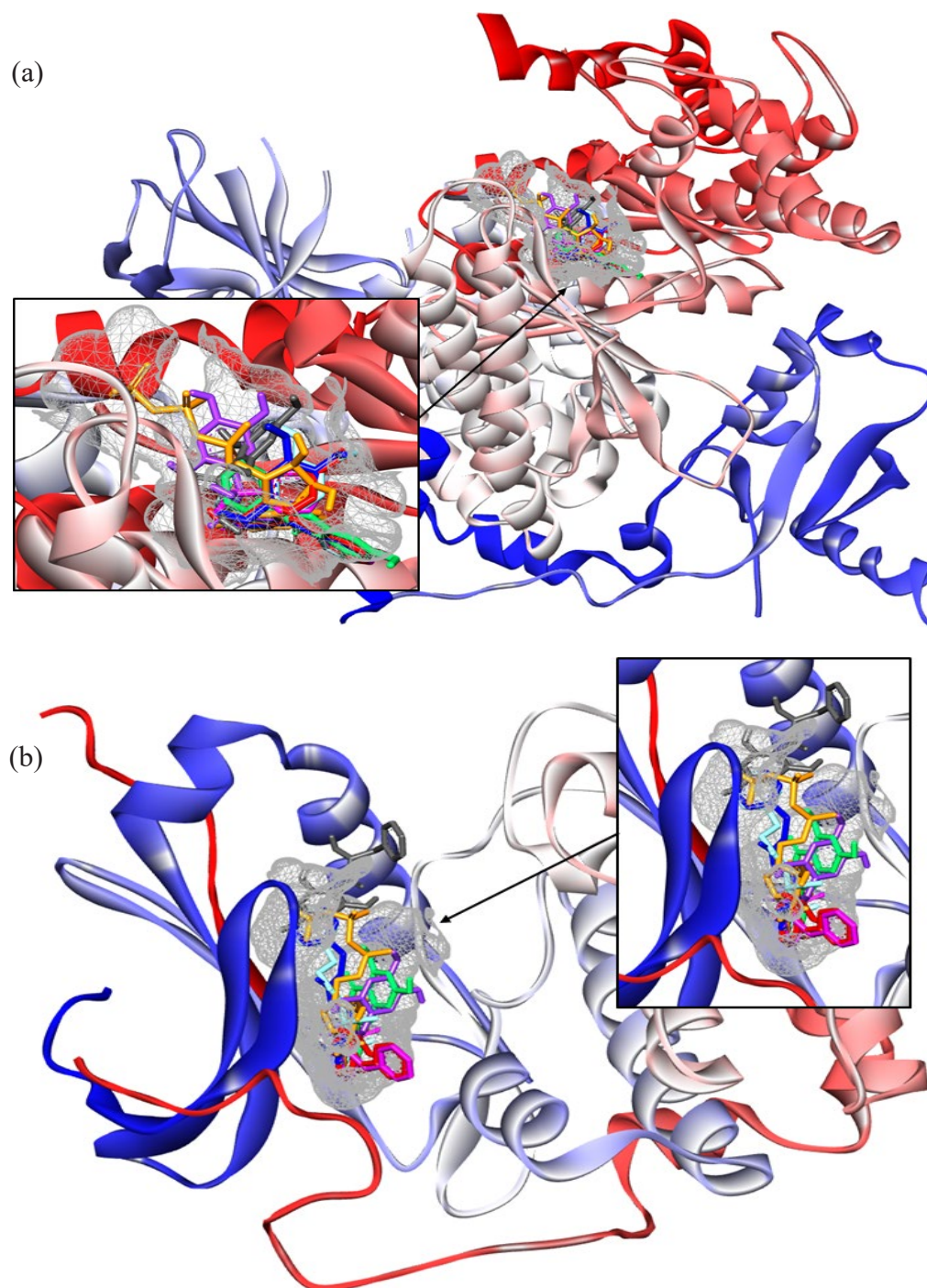


FIGURE 3. Compounds 1 (grey), 2 (red), 3 (purple), 4 (blue), 5 (light blue), 6 (pink), 7 (green), and ATP (orange) binding at the ATP-binding pocket (mesh) of (a) PI3K and (b) AKT1

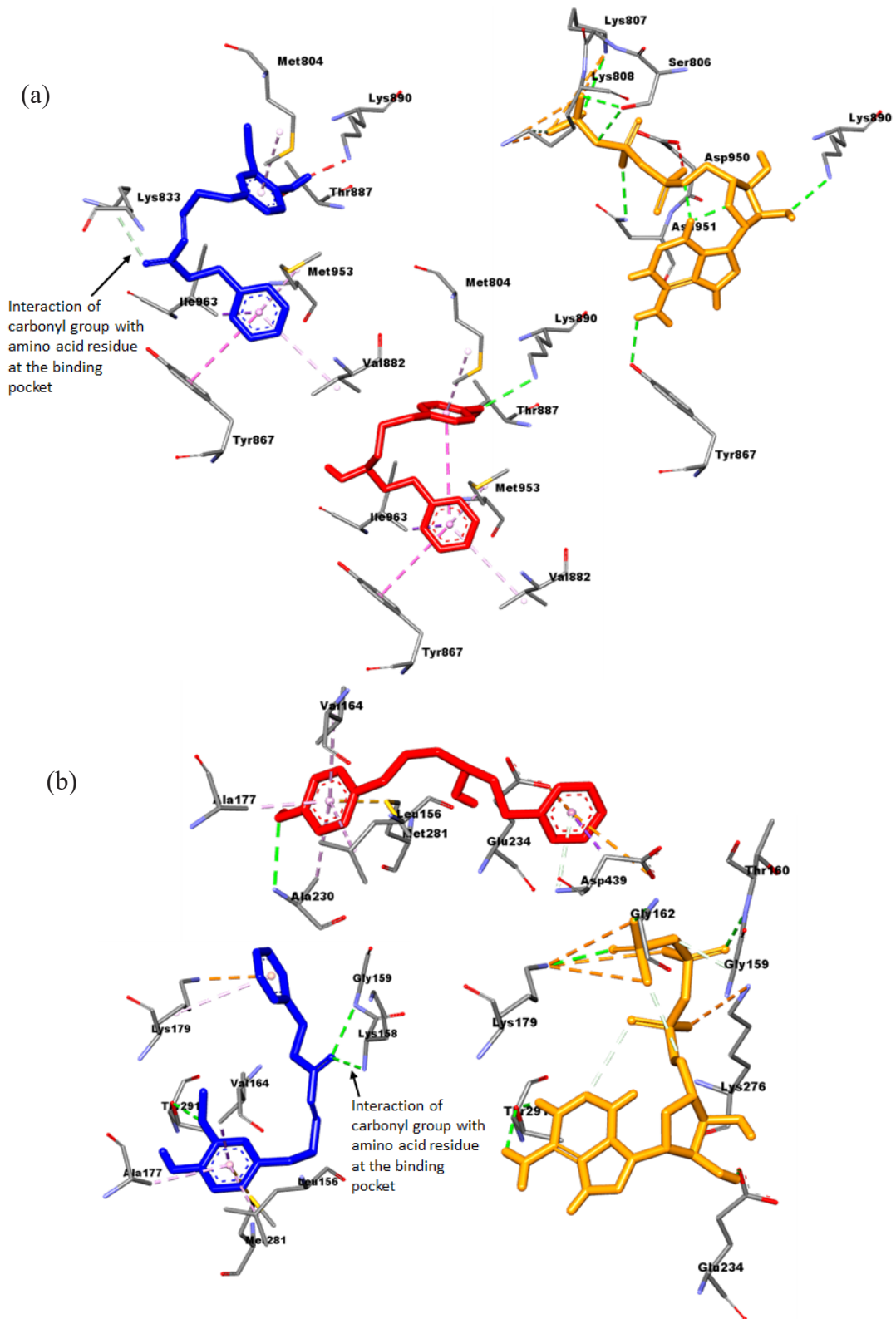


FIGURE 4. Interaction of 2 (red), 4 (blue), and ATP (orange) with the binding pocket amino acid residues of (a) PI3K and (b) AKT1

## CONCLUSIONS

Six compounds bearing the diarylalkanoid structures and one flavonoid, i.e. Stenophyllol A-C (**1-3**), 7-(4-hydroxy-3-methoxyphenyl)-1-phenylhept-4-en-3-one (**4**), and 5*R*-hydroxy-7-(4-hydroxy-3-methoxyphenyl)-1-phenylheptan-3-one (**5**), 1,7-diphenylhept-4-en-3-one (**6**), and 3,5,7-trihydroxyflavone (**7**), have been isolated and characterized from the rhizome of *B. stenophylla*. Compounds **4** and **2** displayed anti-neuroblastoma activity, which reduces the cancerous cell viability to below 20 and 30% within 24 h, respectively. Molecular docking experiments on four protein kinase targets (PI3K, AKT1, ALK, and FAK) responsible for neuroblastoma cell survival have been performed on compounds **1-7** in the effort to understand the possible cause of the anti-neuroblastoma activity. Compounds **2** and **4-7** showed good binding to PI3K and AKT1, suggesting their potential role as protein kinase-inhibitor. The molecular docking results of **2** and **4** are consistent with *in vitro* results, indicating the observed reduction of neuroblastoma cell-viability could be due to the inhibitory effect of **2** and **4** against PI3K and/or AKT1. Our findings also showed the aryl groups in the diarylheptanoid structure could form multiple interactions with the binding pocket amino acid residues and the carbonyl function at the heptanyl middle-chain provided for additional binding interactions with the amino acid residues at the binding pocket. We are confident that the present findings will provide new information for future researchers working on drug design and synthesis.

## ACKNOWLEDGEMENTS

We would like to thank the Chemistry Department and Infra Laboratory Services, University of Malaya for the NMR and MS analysis. This work has been supported by the University of Malaya Grant No. GPF055B-2018, ST004-2018, and ST008-2020. We are grateful to Madam Najmiyah Mohamad Alias from Delima Jelita Herbs Sdn. Bhd. for plant material identification.

## REFERENCES

- Afolayan, A. & Meyer, J. 1997. The antimicrobial activity of 3, 5, 7-trihydroxyflavone isolated from the shoots of *Helichrysum aureonitens*. *Journal of Ethnopharmacology* 57(3): 177-181.
- Ahmad, F.B. & Jantan, I.B. 2003. The essential oils of *Boesenbergia stenophylla* RM Sm. as natural sources of methyl (E)-cinnamate. *Flavour and Fragrance Journal* 18(6): 485-486.
- Bahmad, H.F., Chamaa, F., Assi, S., Chalhoub, R.M., Abou-Antoun, T. & Abou-Kheir, W. 2019. Cancer stem cells in neuroblastoma: Expanding the therapeutic frontier. *Frontiers in Molecular Neuroscience* 12(1): 131.
- Berman, H.M., Westbrook, J., Feng, Z., Gilliland, G., Bhat, T.N., Weissig, H., Shindyalov, I.N. & Bourne, P.E. 2000. The protein data bank. *Nucleic Acids Research* 28(1): 235-242.
- Burley, S.K., Berman, H.M., Bhikadiya, C., Bi, C., Chen, L., Di Costanzo, L., Christie, C., Dalenberg, K., Duarte, J.M., Dutta, S., Feng, Z., Ghosh, S., Goodsell, D.S., Green, R.K., Guranovic, V., Guzenko, D., Hudson, B.P., Kalro, T., Liang, Y., Lowe, R., Namkoong, H., Peisach, E., Periskova, I., Prlic, A., Randle, C., Rose, A., Rose, P., Sala, R., Sekharan, M., Shao, C., Tan, L., Tao, Y.P., Valasatava, Y., Voigt, M., Westbrook, J., Woo, J., Yang, H., Young, J., Zhuravleva, M. & Zardecki, C. 2019. RCSB Protein Data Bank: Biological macromolecular structures enabling research and education in fundamental biology, biomedicine, biotechnology and energy. *Nucleic Acids Research* 47(D1): D464-D474.
- Gabarra-Niecko, V., Schaller, M.D. & Dunty, J.M. 2003. FAK regulates biological processes important for the pathogenesis of cancer. *Cancer and Metastasis Reviews* 22(4): 359-374.
- Gamre, S., Tyagi, M., Chatterjee, S., Patro, B.S., Chattopadhyay, S. & Goswami, D. 2021. Synthesis of bioactive diarylheptanoids from *Alpinia officinarum* and their mechanism of action for anticancer properties in breast cancer cells. *Journal of Natural Products* 84(2): 352-363.
- Greengard, E.G. 2018. Molecularly targeted therapy for neuroblastoma. *Children* 5(10): 142.
- Grosso, D.F., De Mariano, M., Passoni, L., Luksch, R., Tonini, G.P. & Longo, L. 2011. Inhibition of N-linked glycosylation impairs ALK phosphorylation and disrupts pro-survival signaling in neuroblastoma cell lines. *BMC Cancer* 11(1): 525-533.
- Gross, S., Rahal, R., Stransky, N., Lengauer, C. & Hoefflich, K.P. 2015. Targeting cancer with kinase inhibitors. *The Journal of Clinical Investigation* 125(5): 1780-1789.
- Hennessy, B.T., Smith, D.L., Ram, P.T., Lu, Y. & Mills, G.B. 2005. Exploiting the PI3K/AKT pathway for cancer drug discovery. *Nature Reviews Drug Discovery* 4(12): 988-1004.
- Itokawa, H., Morita, M. & Mihashi, S. 1981. Two new diarylheptanoids from *Alpinia officinarum* Hance. *Chemical and Pharmaceutical Bulletin* 29(8): 2383-2385.
- Jänne, P.A., Gray, N. & Settleman, J. 2009. Factors underlying sensitivity of cancers to small-molecule kinase inhibitors. *Nature Reviews Drug Discovery* 8(9): 709-723.
- Johnsen, J.I., Segerström, L., Orrego, A., Elfman, L., Henriksson, M., Kågedal, B., Eksborg, S., Sveinbjörnsson, B. & Kogner, P. 2008. Inhibitors of mammalian target of rapamycin downregulate MYCN protein expression and inhibit neuroblastoma growth *in vitro* and *in vivo*. *Oncogene* 27(20): 2910-2922.
- Karan, D., Dubey, S., Pirisi, L., Nagel, A., Pina, I., Choo, Y.M. & Hamann, M.T. 2020. The marine natural product manzamine a inhibits cervical cancer by targeting the SIX1 protein. *Journal of Natural Products* 83(2): 286-295.

- Ling, J.J., Mohamed, M., Rahmat, A. & Abu Bakar, M.F. 2010. Phytochemicals, antioxidant properties and anticancer investigations of the different parts of several gingers species (*Boesenbergia rotunda*, *Boesenbergia pulchella* var *attenuata* and *Boesenbergia armeniaca*). *Journal of Medical Plants Research* 4(1): 27-32.
- London, W.B., Castleberry, R.P., Matthay, K.K., Look, A.T., Seeger, R.C., Shimada, H., Thorner, P., Brodeur, G., Maris, J.M., Reynolds, C.P. & Cohn, S.L. 2005. Evidence for an age cutoff greater than 365 days for neuroblastoma risk group stratification in the Children's Oncology Group. *Journal of Clinical Oncology* 23(27): 6459-6465.
- Maris, J.M., Hogarty, M.D., Bagatell, R. & Cohn, S.L. 2007. Neuroblastoma. *Lancet* 369(1): 2106-2120.
- Megison, M.L., Gillory, L.A. & Beierle, E.A. 2013. Cell survival signaling in neuroblastoma. *Anti-cancer Agents in Medicinal Chemistry* 13(4): 563-575.
- Mustahil, N.A. 2009. Studies on the chemical compositions and biological activities of essential oils of *Boesenbergia* spp. PhD Thesis. Universiti Malaysia Sarawak (Unpublished).
- Newman, M., Lhuillier, A. & Poulsen, A.D. 2004. Checklist of the zingiberaceae of Malesia. *Blumea. Supplement* 16: 1-166.
- Noor Atiekah Md Nor & Halijah Ibrahim. 2018. Chemical constituents of essential oils of *Boesenbergia armeniaca* and *B. stenophylla* (zingiberaceae) endemic to Borneo. *Pakistan Journal of Botany* 50(5): 1917-1922.
- Primus, P.S., Ismail, M.H., Adnan, N.E., Wu, C.H., Kao, C.L. & Choo, Y.M. 2021. Stenophyllols A-C, new compounds from *Boesenbergia stenophylla*. *Journal of Asian Natural Products Research* 24(2): 146-152.
- Saensouk, S. & Larsen, K. 2001. *Boesenbergia baimaii*, a new species of Zingiberaceae from Thailand. *Nordic Journal of Botany* 21(6): 595-598.
- Sanner, M.F. 1999. Python: A programming language for software integration and development. *Journal of Molecular Graphics and Modelling* 17(1): 57-61.
- Sudsai, T., Prabpai, S., Kongsaree, P., Wattanapiromsakul, C. & Tewtrakul, S. 2014. Anti-inflammatory activity of compounds from *Boesenbergia longiflora* rhizomes. *Journal of Ethnopharmacology* 154(2): 453-461.
- Tewtrakul, S., Subhadhirasakul, S., Puripattanavong, J. & Panphadung, T. 2003. HIV-1 protease inhibitory substances from the rhizomes of *Boesenbergia pandurata* Holtt. *Songklanakarin Journal of Science and Technology* 25(4): 503-508.
- Tori, M., Hashimoto, A., Hirose, K. & Asakawa, Y. 1995. Diarylheptanoids, flavonoids, stilbenoids, sesquiterpenoids and a phenanthrene from *Alnus maximowiczii*. *Phytochemistry* 40(4): 1263-1264.
- Trott, O. & Olson, A.J. 2010. AutoDock Vina: Improving the speed and accuracy of docking with a new scoring function, efficient optimization and multithreading. *Journal of Computational Chemistry* 31(2): 455-461.
- Tuchinda, P., Reutrakul, V., Claeson, P., Pongprayoon, U., Sematong, T., Santisuk, T. & Taylor, W.C. 2002. Anti-inflammatory cyclohexenyl chalcone derivatives in *Boesenbergia pandurata*. *Phytochemistry* 59(2): 169-173.

\*Corresponding author; email: ymchoo@um.edu.my